PHILOSOPHICAL TRANSACTIONS OF THE ROYAL SOCIETY A

rsta.royalsocietypublishing.org

Research

Cite this article: Xu Y, Nesterenko VF. 2014 Propagation of short stress pulses in discrete strongly nonlinear tunable metamaterials. *Phil. Trans. R. Soc. A* **372**: 20130186. http://dx.doi.org/10.1098/rsta.2013.0186

One contribution of 11 to a Theme Issue 'Shock and blast: celebrating the centenary of Bertram Hopkinson's seminal paper of 1914 (Part 2)'.

Subject Areas:
mechanical engineering, materials science

Keywords:
strongly nonlinear, metamaterial, tunable, sound speed, nitrile, toroidal element

Author for correspondence:
Vitali F. Nesterenko
e-mail: vnesterenko@eng.ucsd.edu

Downloaded from https://royalsocietypublishing.org/ on 04 March 2022

Propagation of short stress pulses in discrete strongly nonlinear tunable metamaterials

Yichao Xu[1] and Vitali F. Nesterenko[1,2]

[1]Department of Mechanical and Aerospace Engineering, and [2]Materials Science and Engineering Program, University of California at San Diego, La Jolla, CA 92093-0411, USA

The propagation of short pulses with wavelength comparable to the size of a unit cell has been studied in a one-dimensional discrete metamaterial composed of steel discs alternating with toroidal nitrile O-rings under different levels of precompression using experiments, numerical simulations and theoretical analysis. This strongly nonlinear metamaterial is more tunable than granular chains composed of linear elastic spherical particles and has better potential for attenuation of dynamic loads. A double power-law relationship for compressed O-rings was found to describe adequately their quasi-static and dynamic behaviour with significantly different elastic moduli. It is demonstrated that the double power-law metamaterial investigated allows a dramatic increase in sound speed and acoustic impedance of three to four times using a moderate force.

1. Introduction

Hopkinson's seminal paper [1] introduced the first experimental method allowing measurements of pressures produced by contact explosion or by bullet impact. His approach was based on two main assumptions, which he recognized very clearly and emphasized in a few places in his paper: (i) the material of the rod is perfectly elastic and (ii) '. . .the wave is long comparable with the diameter. . .' [1, p. 445]. These assumptions are of crucial importance because they secure propagation of the pulse without changing its amplitude and shape, so perfectly transmitting the conditions at the loaded end of the bar along its length and allowing measurements of pressures and time of dynamic events.

© 2014 The Author(s) Published by the Royal Society. All rights reserved.

Royal Society Publishing

Downloaded from https://royalsocietypublishing.org/ on 04 March 2022

However, metamaterials with opposite properties (strongly nonlinear and dispersive) are of great practical importance allowing fast transformation/attenuation of waves generated by impact or contact explosion. For example, granular materials (such as a bed of iron shot) and foams are successfully used to attenuate blast loading precisely due to their ability to transform an incoming high-amplitude short-duration pulse into a longer ramped pulse with significantly smaller amplitude [2,3] or trapping them inside the protective barrier [4,5].

The strongly nonlinear dynamic response of low-dimensional metamaterials (granular chains) has received much attention in recent years, because they provide a natural step from linear and weakly nonlinear to strongly nonlinear wave dynamics [2]. The thorough understanding of pulse propagation in these materials can lead to the development of instruments for focusing or attenuation of high-amplitude pulses valuable, for example, in medical applications like disintegration of kidney stones [6].

Most of the earlier studies on granular materials were focused on elastically rigid low-dimensional metamaterials composed of stainless steel beads. It should be mentioned that the elastic modulus (and long-wavelength sound speed) of a metamaterial composed of elastic spherical particles in the case of zero precompression is zero. Thus, the term 'sonic vacuum' was coined [2]. Sound waves can propagate in these systems if they are precompressed and the sound speed increases very fast with increase in applied precompression. Tunability of these strongly nonlinear systems represents their important difference from perfectly linear elastic materials, giving the possibility for 'acoustic diode' effect [7]. Linear chains composed of other metal and polymer beads such as Teflon [8–10] or steel coated with a soft polymer layer [11] were also investigated. It was demonstrated that new strongly nonlinear solitary waves may propagate in these granular materials, even in the case of polymer (Teflon) or polymer-coated beads (Parylene-C coating). The Hertz type of contact interaction at the contact point is still an acceptable approximation for these beads, though with significantly larger elastic moduli than the corresponding static values.

A new type of strongly nonlinear chains composed of 'soft' toroidal elements (Teflon O-rings) and rigid cylinders has been proposed and investigated [12–15]. The advantages of these metamaterials are based on their stronger than Hertzian-type nonlinearity of interaction force and potential for high energy absorption, which is the basis for current extensive applications of O-rings in engineering [16]. The static deformation of these very crucial elements in many devices is well known [17,18], but the dynamic behaviour of these most common and important elements of machine design is not well investigated and understood.

Our investigation is focused on metamaterials with nitrile O-rings as strongly nonlinear elements, which are much softer than Teflon O-rings, with a smaller speed of signal propagation and with a better potential for higher energy absorption. Nitrile is the most popular O-ring elastomer, with wide applications in the seal industry. Compared with traditional granular chains composed of elastic spherical particles, metamaterials with toroidal O-rings may be more tunable, because they exhibit a highly nonlinear, double power-law dependence of force on deformation in static loading [17,18], though their dynamic behaviour is not well known.

In this paper, we focus on the following aspects of behaviour of the periodic discrete metamaterial composed of steel cylinders and O-rings: (i) their ability to support propagation of short pulses with wavelength comparable to the cell size of the metamaterial, (ii) relevance of strongly nonlinear static force–displacement relations to the dynamic behaviour of O-rings, and (iii) tunability of metamaterial sound speed caused by compressive force.

2. Theoretical analysis

Consider a periodic chain of N steel cylinders separated by nitrile O-rings that are compressed by a static force F_0. One cell contains a stainless steel cylinder and O-ring, as shown in figure 1, and has initial size a ($a = h + d$, where h is the height of the steel cylinder and d is the cross-sectional diameter of an undeformed O-ring). The forces between cylinders are due to nonlinear elastic deformation of O-rings caused by decreasing their height by ε. The quasi-static elastic

Downloaded from https://royalsocietypublishing.org/ on 04 March 2022

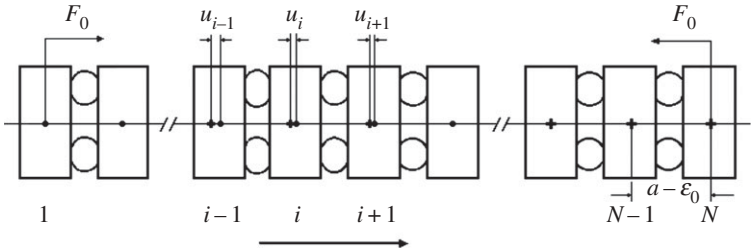

Figure 1. Schematic diagram of one-dimensional metamaterial composed of steel cylinders alternating with nitrile O-rings compressed by a large (in comparison with dynamic force applied as an impulse) static force F_0. The static force causes an initial displacement ε_0 between neighbouring centres of cylinders, u_i is the displacement of the ith cylinder from its equilibrium position in the statically compressed chain and a is the distance between centres of neighbouring cylinders without precompression. The right-hand end of the chain is undisturbed, and the arrow at the bottom shows the direction of pulse propagation. The crosses show the initial equilibrium position of cylinder centres in the statically compressed chain. The black circles correspond to the position of the cylinder centres in the wave.

forces between cylinders (F_{el}) are represented by a double power-law equation and depend on their geometric parameters, elastic properties and the ratio (ε/d) [17,18]

$$F_{\mathrm{el}} = \pi D_{\mathrm{m}} d E_0 \left[1.25 \left(\frac{\varepsilon}{d}\right)^{3/2} + 50 \left(\frac{\varepsilon}{d}\right)^{6} \right], \tag{2.1}$$

where D_{m} is a mean diameter (defined as the inside diameter plus cross-sectional diameter of the O-ring), and E_0 is the quasi-static Young's modulus of the nitrile rubber. Thus, O-rings represent strongly nonlinear elastic elements with nonlinearity stronger than the Hertzian law at relatively large ε, when the second term in equation (2.1) dominates.

The contact deformation of the soft O-ring is confined to a very small region near the contact point with the rigid steel cylinders. As a first approximation, we can consider that deformation of an O-ring during a dynamic process obeys static equation (2.1), because its strong nonlinearity is due mainly to geometrical effects, with the possible change in the elastic modulus E_0 accounting for strain-rate effects. The steel cylinders hardly deform during this process, and it is assumed that the duration of the pulse is much longer than the characteristic time for wave propagation inside the cylinders, which allows us to consider them as point masses. In our investigation, the mass of the steel cylinders ($m = 3.065$ g) was about 50 times larger than that of the O-rings (mass 0.0625 g). Thus, to a first approximation, the O-rings can be considered as massless viscoelastic springs.

It is convenient to introduce the initial height change of the O-ring ε_0 into the equation explicitly. Then the equations of cylinder motion (without considering dissipation) become

$$\ddot{u}_i = A[(\varepsilon_0 - u_i + u_{i-1})^{3/2} - (\varepsilon_0 - u_{i+1} + u_i)^{3/2}] + B[(\varepsilon_0 - u_i + u_{i-1})^6 - (\varepsilon_0 - u_{i+1} + u_i)^6], \tag{2.2}$$

where u_i ($2 \le i \le N-1$) denote the displacement of the ith cylinder from its static equilibrium position in the initially compressed chain, and the O-rings remain compressed during the wave propagation. If we assume that the behaviour of an O-ring obeys the static dependence of force on ε, then $A = 1.25\pi D_{\mathrm{m}} E_0/md^{1/2}$ and $B = 50\pi D_{\mathrm{m}} E_0/md^5$ [17,18]. The dot denotes a derivative with respect to t.

The anharmonic approximation of discrete equations (2.2) in the long-wave limit ($L \gg a_1 = a - \varepsilon_0$, where L is the characteristic spatial size of the wave perturbation, a_1 is the cell size in the preloaded system) can be derived using the continuum variable replacement, resulting in the Boussinesq wave equation [2]

$$u_{tt} = c_0^2 u_{xx} + 2\gamma c_0 u_{xxxx} - \sigma u_x u_{xx}, \tag{2.3}$$

where the subscripts t or x denote the partial derivatives with respect to t or x.

Downloaded from https://royalsocietypublishing.org/ on 04 March 2022

For short pulses, the regularized Boussinesq wave equation is more suitable [2]

$$u_{tt} = c_0^2 u_{xx} + \frac{2\gamma}{c_0} u_{ttxx} - \sigma u_x u_{xx}, \tag{2.4}$$

where the corresponding parameters are

$$c_0^2 = \left(\frac{3A\varepsilon_0^{1/2}}{2} + 6B\varepsilon_0^5\right) a_1^2, \quad \gamma = \frac{c_0 a_1^2}{24} \quad \text{and} \quad \sigma = \left(\frac{3A\varepsilon_0^{-1/2}}{4} + 30B\varepsilon_0^4\right) a_1^3.$$

All the higher-order terms are omitted, and the convective derivative in acceleration is ignored, assuming that the speed of the pulse is much larger than the particle velocity.

The long-wave sound speed c_0 can be expressed as

$$c_0^2 = a_1^2 \left| \frac{3}{2} A(a\xi_0)^{1/2} + 6B(a\xi_0)^5 \right|, \tag{2.5}$$

where ξ_0 is the static initial global strain in the metamaterial, defined as ε_0/a. It is assumed that the dynamic behaviour of the O-ring is similar to its static response.

It should be mentioned that the sound speed c_0 in equation (2.5) is different from the sound speed in the steel cylinder or nitrile O-ring. It is a long-wave sound speed in the whole metamaterial. This can be significantly smaller than the bulk sound speed in the materials of the cylinder or O-ring and can be tuned by precompression. Apparently, the sound speed c_0 not only depends on the initial strain, but also can be affected by the elastic modulus of the O-rings, their geometric parameters and the mass of the steel cylinders.

The dispersion relations for linearized equations (2.3) and (2.4) are, correspondingly,

$$\omega^2 = c_0^2 k^2 - 2c_0 \gamma k^4 \tag{2.6}$$

and

$$\omega^2 = c_0^2 k^2 \left(1 + \frac{2\gamma}{c_0} k^2\right)^{-1}. \tag{2.7}$$

Here k is the wavevector ($2\pi/\lambda$), and λ is the wavelength. Based on the above dispersion relations, the group velocity c_g of a pulse propagating through the chain is given by the following equation for the Boussinesq and regularized Boussinesq wave equations, respectively:

$$c_g \equiv \frac{d\omega}{dk} = c_0 \left(1 - \frac{a_1^2 k^2}{6}\right) \left(1 - \frac{a_1^2 k^2}{12}\right)^{-1/2} \tag{2.8}$$

and

$$c_g \equiv \frac{d\omega}{dk} = c_0 \left(1 + \frac{a_1^2 k^2}{12}\right)^{-3/2}. \tag{2.9}$$

Equation (2.3) could be transformed into the Korteweg–de Vries (KdV) equation under the same assumptions [2,19]

$$\xi_t + c_0 \xi_x + \gamma \xi_{xxx} + \frac{\sigma}{2c_0} \xi \xi_x = 0, \quad \xi = -u_x. \tag{2.10}$$

According to the KdV equation (2.10), a stationary solitary wave and shock wave (if dissipation is included) can propagate in an initially compressed weakly nonlinear system [2,20]. This equation (2.10) could be used to analyse the behaviour of the investigated metamaterial for the weakly nonlinear case, when the force amplitude of the localized pulse is significantly smaller than the initial precompression force. The solitary wave speed V_s is given by

$$V_s = c_0 + \frac{\sigma(\xi_m - \xi_0)}{6c_0}, \tag{2.11}$$

where ξ_m is the maximum strain in the solitary wave.

It is evident that the speed of this wave has a linear dependence on the maximum strain and, in the weakly nonlinear case ($\xi_m - \xi_0 \ll \xi_0$), V_s is close to the sound speed. We use this equation to estimate the role of nonlinearity on the value of the pulse speed for the short compression pulses

Downloaded from https://royalsocietypublishing.org/ on 04 March 2022

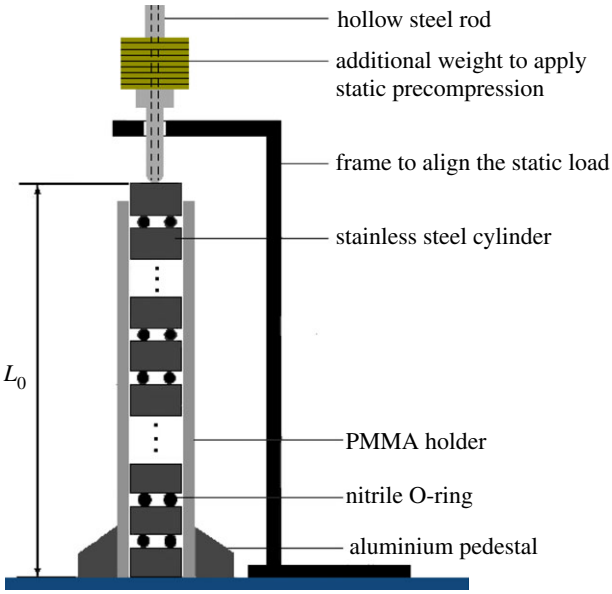

Figure 2. Experimental set-up with 16 O-rings placed between 17 stainless steel cylinders under an applied static load. The frame with a hole inside its upper part keeps the hollow steel rod aligned in vertical direction. (Online version in colour.)

observed in our experiments. It should be mentioned that only compression solitary waves are supported by nonlinear systems with elastic stiffening under compression.

3. Experiments

The behaviour of the O-rings under static deformation was investigated by loading a chain of 17 steel cylinders alternating with 16 nitrile O-rings (N70-008, supplied by O-ring West) using a weight attached to the top; four cylinders and three O-rings were used at smaller static loads $F_0 = 3.1$ N and $F_0 = 8.2$ N to minimize the influence of their weight (figure 2). In our experiments, each O-ring had an initial cross-sectional diameter $d = 1.78$ mm, a mean diameter $D_m = 6.22$ mm and mass $m_0 = 0.0625$ g. They were placed between steel cylinders with height $h = 5.0$ mm, diameter 10.0 mm and mass $m = 3.065$ g. The initial cell size a and height of the system L_0 were equal 6.78 mm and 113.48 mm, respectively.

Figure 3 presents the results of measurements of relative displacements ε of neighbouring steel cylinders at different static compression forces compared with the theoretical value obtained using equation (2.1). Owing to their viscoelastic behaviour, we observed saturation of the deformation of O-rings after about 4 min following the application of load. The measurements were repeated four times for each static load in the range 3.1–193.0 N, and the average values of the multiple measurements are shown in figure 3 with standard deviation in the range of 2–4% for loads 70.3–193.0 N and 5–9% for smaller static loads 3.1–52.2 N.

A very good fit between experimental and calculated data using a double power law with corresponding exponents 3/2 and 6 (equation (2.1)) and elastic modulus $E_0 = 7.6$ MPa (which is close to the value 9 MPa reported for nitrile [21]) was obtained for the range of forces investigated. This is in agreement with experimental and theoretical data for O-rings made from different materials up to $\varepsilon/d = 0.5$ [16]. It is important that the functional dependence of the force on ε/d is significantly different from Hertzian behaviour at $\varepsilon/d > 0.3$ (figure 3).

Stress wave propagation in this metamaterial was investigated using a set-up similar to that shown in figure 2. Two piezo-sensors (supplied by Piezo Systems, Inc.; 6 mm side plates with 0.267 mm thickness, RC of the electrical circuit approx. 5.24 ms) were embedded in the fifth and the ninth cylinders (from the top) similar to the study of Daraio *et al.* [10]. Sensors were

Downloaded from https://royalsocietypublishing.org/ on 04 March 2022

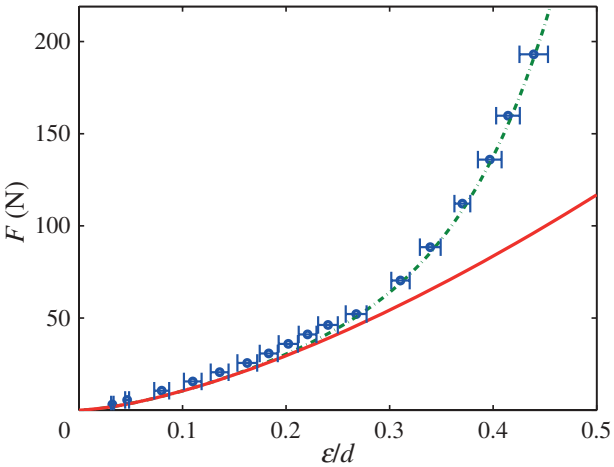

Figure 3. Experimental and theoretical values of global strain in O-ring as function of static forces. The dashed (green) line represents the theoretical curve corresponding to equation (2.1) with $E_0 = 7.6$ MPa, and the solid (red) line denotes the corresponding Hertzian part ($n = 3/2$) of the force at $E_0 = 7.6$ MPa. The experimental values are shown by (blue) circles. (Online version in colour.)

calibrated using conservation of linear momentum in separate impact experiments. Signals from these gauges were detected using a digital Tektronix oscilloscope (TDS 2014). Small-amplitude pulses (with positive and negative amplitudes being less than 10% of the precompression force), whose speed can be identified with the sound speed under various precompression forces, were generated by impacts of a steel sphere (0.455 g) with a velocity of $2.62\,\mathrm{m\,s^{-1}}$ moving inside a hollow steel rod.

The shapes of the pulses are presented in figure 4 for the smallest and the largest precompression forces. The zero time in the figures is arbitrary.

We calculated the speed of the positive and negative phases of pulses by dividing the distance between the sensors $4a_1$ by the measured peak-to-peak time interval. The accuracy of speed measurement was within 10% or better (depending on the precompression force) and within this limit the speeds of positive and negative pulses were close, demonstrating weak dispersion. The speed data are shown in table 1.

The recorded pulses change their shape (e.g. ramping of leading fronts, total length of pulse increased from 500 to 700 µs in figure 4*a*), and this was mainly caused by dissipation. The combined spatial widths of positive and negative phases of pulses (L_{exp}, table 1) were calculated based on their speeds and durations as detected by the gauge in the fifth cylinder.

One of the distinguishing features of the highly nonlinear metamaterial investigated is the strong tunability of pulse speed using initial precompression. Because the amplitude of the pulses was much smaller than the initial precompression, the speed of pulses was close to the sound speed in the continuum limit based on equation (2.11). Thus, we may use the equation for sound speed to estimate the theoretical speed of these pulses. The comparison of experimental results and theoretical values for the sound speed using equation (2.5), assuming that the dynamic behaviour of the O-rings obeys the static dependence of force on ε/d with $E_0 = 7.6$ MPa, is shown in figure 5.

From figure 5, we can see that the values of pulse speed are significantly larger than the predicted values based on the static elastic modulus $E_0 = 7.6$ MPa. It should be mentioned that the theoretical calculations do take into account the strong nonlinearity, resulting in the increase of sound speed, as is evident from the behaviour of curve 1, but the calculated numerical values are too low. It is also evident that the behaviour of the experimental data does not reflect even qualitatively the sound speed behaviour based on Hertz's law (curve 2). Rather, it demonstrates a more pronounced dependence of signal speed on initial precompression,

Downloaded from https://royalsocietypublishing.org/ on 04 March 2022

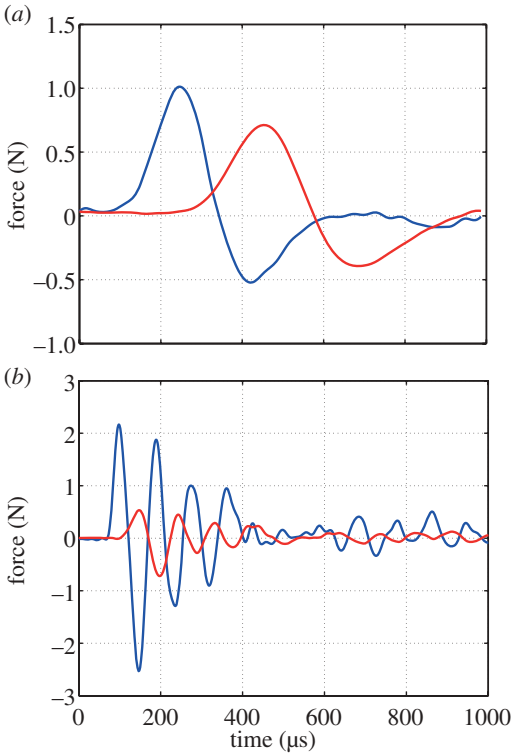

Figure 4. Stress pulses in a chain of nitrile O-rings and stainless steel cylinders generated by a steel striker (0.455 g) with an initial velocity of 2.62 m s^{-1}: static precompression force (*a*) 10 N and (*b*) 193 N. Sensors placed in the fifth and the ninth cylinders recorded the average dynamic forces in them. (Online version in colour.)

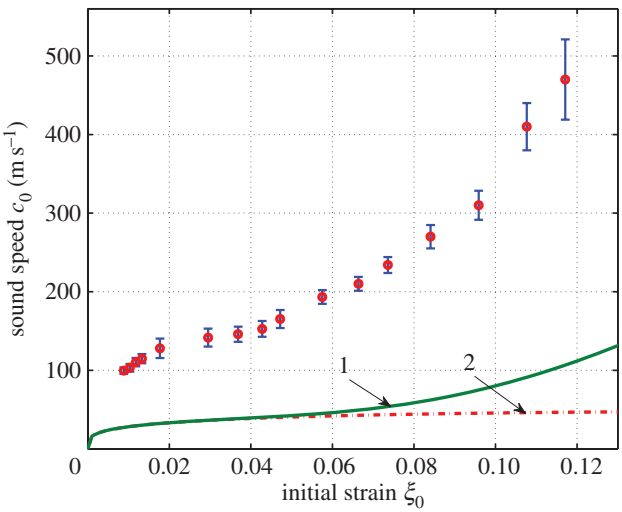

Figure 5. Experimental and theoretical dependence of sound speed on initial strain for double power-law system. The experimental values of pulse speed are shown by (red) circular dots. Curve 1 (green) represents the long-wave sound speed (equation (2.5)) with $E_0 = 7.6$ MPa. Curve 2 (dashed red) represents sound speeds corresponding to the Hertzian part of the interaction law with single exponents 3/2 at $E_0 = 7.6$ MPa. (Online version in colour.)

Downloaded from https://royalsocietypublishing.org/ on 04 March 2022

Table 1. Speeds of positive pulses (V_+) and combined widths of positive and negative pulses (L_{exp}) for different precompression forces detected in experiments corresponding to the signal recorded by gauges embedded in the fifth and the ninth cylinders.

F_0 (N)	V_+ (m s^{-1})	L_{exp}/a_1
10	128 ± 13	9
30	165 ± 12	7
50	210 ± 9	7
74	270 ± 9	7
106	310 ± 9	6
193	468 ± 28	7

characteristic of the behaviour of sound speed for a double power-law interaction. It should be mentioned that the dynamic rigidity of this system may be significantly influenced by viscoelastic behaviour, as is evident from the pulse attenuation especially in the case of a large precompression force (figure 4*b*).

We can also see that a Hertzian-type interaction is beneficial for the tuning of sound speed only for a low range of initial strain. The part of the interaction law with exponent equal to 6 makes metamaterials more tunable at large strains (this transition of qualitative behaviour of sound speed with precompression happens for values of $\xi_0 > 0.06$; figure 5).

Thus, we apparently need to take into account that O-rings behave differently under dynamic deformation by waves in comparison with static deformation.

To clarify the dynamic behaviour of the metamaterial investigated, we proceed with the analysis using numerical calculations of the discrete system.

4. Numerical calculations

Numerical calculations representing the experimental set-up shown in figure 2 were performed using MATLAB. The steel cylinders were treated as rigid bodies connected by massless nonlinear springs representing the O-rings, with deformation behaviour following a strongly nonlinear double power law (dissipation was not included). To model the static precompression force, we introduced gravitational forces applied to the large top mass (hollow steel rod plus additional weight). It is assumed that there is a Hertzian-type interaction at the contact of the hollow steel rod (connected to the precompression mass) and the top cylinder in the chain. Gravitational force was also applied to all particles, simulating conditions in the experiment, though results of numerical modelling demonstrated that gravitational forces acting on particles did not affect the speed of the signals in the investigated range of precompression forces and pulse amplitudes. The pulses were excited by a steel impactor and we assume Hertzian-type elastic interaction between impactor and the top steel cylinder in the chain.

In the numerical calculations, we consider that the displacement ε between neighbouring cylinders relative to their positions in the undeformed chain is equal to the initial value ε_0 plus an additional small change during dynamic deformation ε_d. In our experimental conditions, the system is initially strongly compressed and the dynamic part ε_d of the decrease in the height of the O-rings is much smaller than ε_0. Thus, we can approximate the dynamic contribution to the force by a linear function of ε_d, so that total force due to the deformation of an O-ring becomes

$$F_{el} = A_0 m \varepsilon_0^{3/2} + B_0 m \varepsilon_0^6 + K \varepsilon_d, \tag{4.1}$$

where $A_0 = 1.25\pi D_m E_0/md^{1/2}$ and $B_0 = 50\pi D_m E_0/md^5$. We observed in experiments that the speed of the signals increases nonlinearly with precompression (figure 5 and table 1). Thus, the coefficient K should have a nonlinear dependence on the initial precompression. It should be mentioned that effective elastic moduli have been successfully used for the dynamic contact behaviour of viscoelastic beads (nylon [9], PTFE [10]) or beads coated with a polymer layer [11].

Downloaded from https://royalsocietypublishing.org/ on 04 March 2022

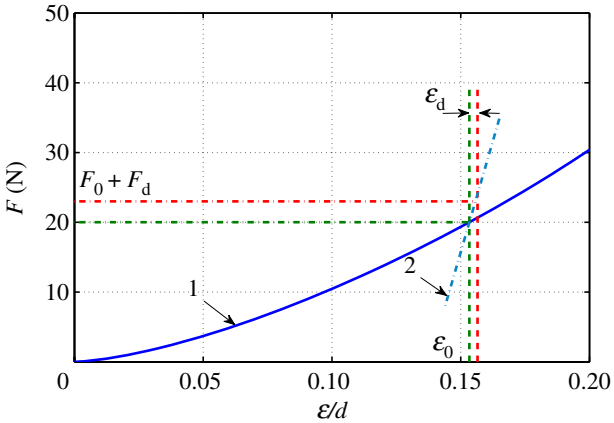

Figure 6. The difference in dynamic behaviour of O-ring in comparison with static conditions. Curve 1 (blue) represents a relationship according to a double power law at $E = 7.6$ MPa. The initial relative displacement of neighbouring steel cylinders is ε_0, and its small change during dynamic deformation is ε_d. Curve 2 (dashed blue) corresponds to linear dynamic part in equation (4.1) with coefficient K represented by equation (4.2), which includes dependence on ε_0. (Online version in colour.)

We assume that this coefficient can also be found based on a double power-law relationship (which is of geometrical origin), with the effective elastic modulus E_d reflecting the dynamic deformation of the viscoelastic O-rings. Thus, we introduce the following dependence of the coefficient K on static precompression, which is based on a linearized version of the double power law (equation (2.1)) in the vicinity of ε_0, but with dynamic value for the elastic modulus E_d,

$$K = 1.5(1.25\pi D_m E_d d^{-1/2})\varepsilon_0^{1/2} + 6(50\pi D_m E_d d^{-5})\varepsilon_0^5. \tag{4.2}$$

The coefficient K depends both on the dynamic modulus (E_d) of the nitrile O-rings and on the system's initial deformation ε_0. As illustrated in figure 6, the dynamic force at a given ε_d may deviate significantly from the static curve depending on the selected value of E_d. The value of the effective dynamic modulus of the O-rings E_d is a fitting parameter, which includes increased stiffness due to elastic and viscous behaviour to match the speed of signals detected in experiments with the results of numerical calculations.

A chain of 40 elements is used in the numerical calculations. The second-order differential equations for particles inside the chain were reduced to the first-order equations [2]

$$\dot{x}_i = F_i(\bar{x}), \quad \bar{x} = (x_1, x_2, \ldots, x_{2N}), \quad i = 1, \ldots, 2N,$$

$$F_i(\bar{x}) = x_{N+i}, \quad i = 1, \ldots, N-1,$$

$$F_i(\bar{x}) = \varphi_i(\bar{x}) - \psi_i(\bar{x}) + g, \quad i = N+1, \ldots, 2N-1,$$

$$\varphi_i(\bar{x}) = 0, \quad i = N+1, N+2,$$

$$\varphi_i(\bar{x}) = \frac{C}{m}\delta_{i-2-N,i-N}^{3/2} H(\delta_{i-2-N,i-N}) + \frac{D}{m}\delta_{i-1-N,i-N}^{3/2} H(\delta_{i-1-N,i-N}), \quad i = N+3,$$

$$\varphi_i(\bar{x}) = [A_0(x_{0,i-1-N})^{3/2} + B_0(x_{0,i-1-N})^6 + \frac{K_{i-1-N}}{m}(\delta_{i-1-N,i-N} - x_{0,i-1-N})]H(\delta_{i-1-N,i-N}),$$

$$i = N+4, \ldots, 2N-1,$$

$$\psi_i(\bar{x}) = \frac{C}{M}\delta_{i-N,i+2-N}^{3/2} H(\delta_{i-N,i+2-N}), \quad i = N+1,$$

$$\psi_i(\bar{x}) = \frac{D}{m_{imp}}\delta_{i-N,i+1-N}^{3/2} H(\delta_{i-N,i+1-N}), \quad i = N+2,$$

Downloaded from https://royalsocietypublishing.org/ on 04 March 2022

Table 2. Speeds of positive pulses (V_+) and combined widths of positive and negative pulses (L_{num}) for different precompression forces detected in numerical calculations corresponding to the dynamic forces acting on the fifth and the ninth cylinders.

F_0 (N)	V_+ (m s^{-1})	L_{num}/a_1
10	127	7
30	156	6
50	189	6
74	237	6
106	286	6
193	390	6

$$\psi_i(\bar{x}) = \left[A_0(x_{0,i-N})^{3/2} + B_0(x_{0,i-N})^6 + \frac{K_{i-N}}{m}(\delta_{i-N,i+1-N} - x_{0,i-N})\right] H(\delta_{i-N,i+1-N}),$$

$$i = N+3, \ldots, 2N-1$$

and $\delta_{i-2-N,i-N} = x_{i-2-N} - x_{i-N}$.

Boundary conditions are

$$F_i(\bar{x}) = 0, \quad i = N, 2N.$$

Initial conditions corresponding to gravitationally loaded chain are

$$x_N(t=0) = 0, \quad x_{N-i}(t=0) = x_{N-i+1}(t=0) + x_{0,N-i}, \quad i = 1, \ldots, N-2,$$

$$x_1(t=0) = x_3(t=0) + x_{0,1},$$

$$x_{N+1}(t=0) = 0, \quad x_{N+2}(t=0) = 2.62, \quad x_{N+i}(t=0) = 0, \quad 2 < i \leq N,$$

and $K_{i-1-N} = 1.5(1.25\pi D_{\mathrm{m}} E_{\mathrm{d}} d^{-1/2}) x_{0,i-1-N}^{1/2} + 6(50\pi D_{\mathrm{m}} E_{\mathrm{d}} d^{-5}) x_{0,i-1-N}^5, \quad i = N+4, \ldots, 2N.$

The values of x_i for $i = 1, \ldots, N$ are the displacement of the ith particle from its equilibrium position (corresponding to the chain before it was deformed by gravitational forces, $g = 9.81\ \mathrm{m\,s^{-2}}$ is the gravitational acceleration) assumed due to static loading and dynamically, while x_i for $i = N+1, \ldots, 2N$ is the velocity of the ith particle. The Heaviside function $H(\delta)$ ensures that interactions exist only when the grains are in contact ($\delta > 0$). The coefficients C and D represent nonlinear Hertzian-type interactions between the precompressing mass (particle 1) and the top steel cylinder (particle 3) and between the impactor (particle 2) and the top cylinder. The precompressing mass and impactor have mass M and m_{imp}, respectively.

It should be noted that $x_{0,1}$ is the initial displacement of the precompressing mass with respect to the first cylinder assuming gravitational loading, while $x_{0,2} = 0$ and $x_{0,i}$ ($i = 3, \ldots, N-1$) are the changes of the initial height of the O-ring between the ith and $(i+1)$th cylinder introduced by gravitation. The values of the initial displacements produced by gravitational loading are calculated by using equation (2.1) with the static O-ring modulus $E_0 = 7.6$ MPa.

The results of numerical calculations modelling dynamic experiments are presented in table 2.

The corresponding pulses shown in figure 7 for elastic modulus $E_{\mathrm{d}} = 105$ MPa provide the best fit of the experimental data and the results of numerical calculations (figure 8). The zero time in the numerical calculations corresponds to the moment of impact.

The speeds of positive and negative pulses in the numerical calculations were close (the speeds of negative pulses were smaller by about 6–17% for small and large values of compression forces). The dispersion effects are evident in figure 7, but they did not dramatically change the amplitude and shape of pulses at the distances investigated, and this is consistent with the expected weak dispersion based on equations (2.8) and (2.9). Fourier spectra of propagated pulses, detected in corresponding locations, were similar.

Downloaded from https://royalsocietypublishing.org/ on 04 March 2022

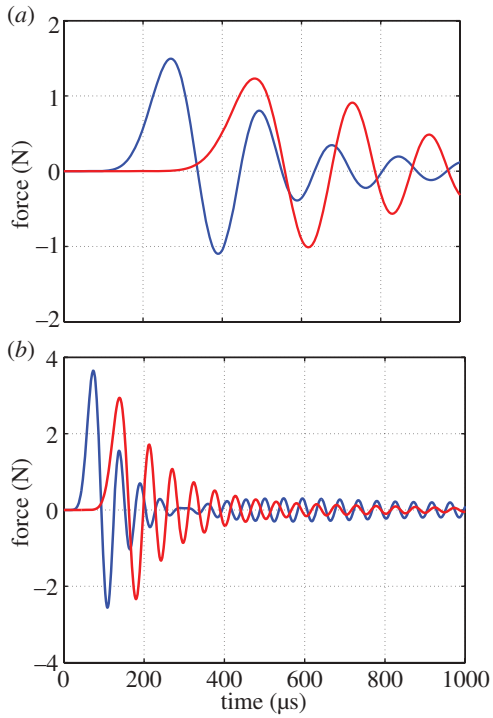

Figure 7. Stress pulses in a chain of nitrile O-rings and stainless steel cylinders generated by a steel striker (0.455 g) with an initial velocity of 2.62 m s^{-1}: static precompression force (*a*) 10 N and (*b*) 193 N. The numerically generated curves represent average dynamic force in the fifth and the ninth cylinders corresponding to the experimental data presented in figure 4. (Online version in colour.)

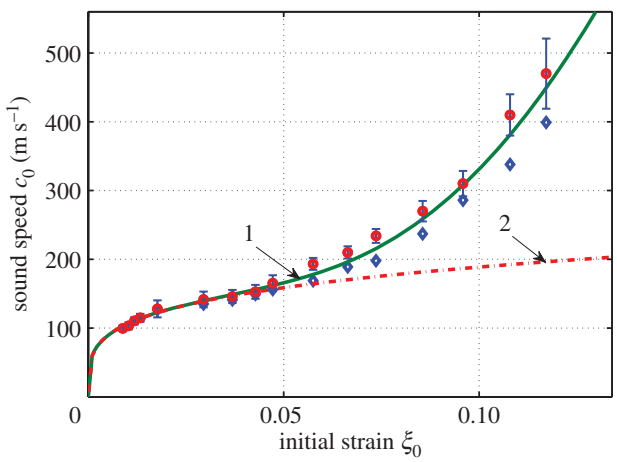

Figure 8. Experimental (red circles) and numerical (blue diamonds) dependence of pulse speed on initial strain for metamaterial investigated. Curve 1 (green) represents the long-wave sound speed (equation (2.5)) at $E_0 = 105$ MPa. Curve 2 (dashed red) represents sound speeds corresponding to the Hertzian part of the interaction law with single exponents 3/2 at $E_0 = 105$ MPa. (Online version in colour.)

The cause of the negative phase of the pulses (similar to that observed in other work [8,22]) is the reduction of the initial static precompression force due to the motion of the first cylinder with respect to the hollow steel rod attached to the precompressing mass.

Downloaded from https://royalsocietypublishing.org/ on 04 March 2022

It is interesting to compare the theoretical value of the sound speed (equation (2.5)) based on the assumed effective modulus of the O-ring $E_d = 105$ MPa with the results of numerical calculations, as well as with experimental data. The corresponding data are shown in figure 8.

5. Discussion

Experimental data for static deformation of nitrile O-rings confirmed their strongly nonlinear behaviour, with the elastic modulus $E_0 = 7.6$ MPa being consistent with results reported for these elements [17,18].

Experiments have shown that this metamaterial is highly tunable: the static force increases from 10 to 193 N, resulting in the increase of signal speed by more than a factor of 3 with a decrease in pulse duration and spatial length under the same method of pulse excitation (figure 4 and table 1).

There is a large difference between the experimental data and the predicted speed of sound based on equation (2.5), if we use a static value of the elastic modulus $E_0 = 7.6$ MPa (figure 5). The spatial length of our signals is comparable to the cell size. Thus, we can expect the influence of linear dispersion on phase speed. But according to equation (2.9) linear dispersion can only slightly reduce (not increase) the signal speed to $0.91c_0$ at the wavelength in the experiments close to $7a_1$. Thus, we cannot attribute the difference between the predicted values of c_0 and measurements as being due to dispersion.

From another point of view, we measure the velocity of signals with finite amplitude. Thus, nonlinearity may increase the speed of propagation in comparison with the sound speed. The role of nonlinearity can be estimated based on the speed of solitary waves at a given amplitude (a solitary wave represents a balance of dispersion and nonlinearity). Based on this estimate, nonlinearity can increase the speed of propagation to at most $1.03c_0$ (at an initial precompression force $F_0 = 10$ N) assuming that the positive phase of the pulse is approximated by a solitary wave (equation (2.11)). Clearly, weak nonlinearity is not able to explain the large discrepancy between experimental data and the theoretical value of c_0 based on the extension of the quasi-static behaviour of O-rings ($E_0 = 7.6$ MPa) into the dynamic regime.

From the numerical data, we can see that, despite the short length of pulses, dispersion effects did not dramatically change the amplitude, shape and spectrum of propagating pulses at the distances investigated. This is in agreement with estimates based on a continuum approximation (equations (2.8) and (2.9)). Changes of shape and amplitude of pulses in experiments are mostly due to dissipation, which will be considered in a separate publication. The speeds of pulses in numerical calculations for $E_d = 105$ MPa are close to the corresponding experimental values (figure 8). A continuum equation for long-wave sound speed (equation (2.5)) with elastic modulus $E_d = 105$ MPa satisfactorily describes the speed of pulses in experiments and in numerical calculations (figure 8). The slight differences between numerical data and theoretical values based on equation (2.5) for sound speed might be due to dispersion effects.

The value of this effective dynamic modulus $E_d = 105$ MPa is considerably higher than the value obtained from static experiments (approx. 7.6 MPa), which is qualitatively similar to the dynamic behaviour of Teflon and Parylene-C [8–11]. We did not separate inputs of elastic and viscous components in this increased stiffness, though the role of dissipation is significant in experiments. The increased value of the effective elastic modulus may be due to the material strain-rate sensitivity of nitrile rubber, and the selected value of E_d is characteristic only for the conditions of our experiments. In this study, the local static strains in the O-rings in our experiments were up to 0.44, the global dynamic strains in our numerical calculations lay in the interval 3×10^{-3} to 9×10^{-4} and the corresponding strain rates were approximately 30–27 s^{-1}.

The deformation behaviour of polymer toroidal O-rings is path-sensitive and, in high strain, strain-rate dynamic deformation (without initial precompression) can be successfully described by a strongly nonlinear viscoelastic model [23], also demonstrating increase of stiffness in dynamic conditions.

Downloaded from https://royalsocietypublishing.org/ on 04 March 2022

The detailed explanation of dramatic increase of dynamic stiffness of O-rings requires investigation of their dynamic contact deformation concentrated in a very small area with large local strains and their gradients. The mechanism of this dramatic increase of stiffness of O-rings is the focus of our future research.

6. Conclusion

The speed of sound waves in metamaterial was used to measure the dynamic properties of strongly nonlinear elements (O-rings). Such measurements can be difficult to conduct for very small elements, like very small O-rings or thin layers of nanofoams. At the same time, the measurements of the sound speed related to the dynamic stiffness of deformed elements in the system (in our case O-rings) can be accomplished irrespective of their size, because it is based on the measurements of wave speed on macroscopic distances.

The propagation of small-amplitude short-duration pulses in a one-dimensional strongly nonlinear metamaterial was investigated for different conditions of static preloading by both experiment and numerical calculation. They have a speed that significantly exceeds the speed of sound estimated based on the quasi-static behaviour of O-rings. The large discrepancy is explained by a dramatic increase in effective stiffness of precompressed O-rings under dynamic deformation by the wave. This demonstrates that the design of O-rings, which are very important elements with widespread use in machinery, should take into account their dramatic increase of rigidity under dynamic conditions even at low velocity of impact.

It was shown that signal speed in this double power-law metamaterial is a few times more tunable at higher preload than sound speed in granular chains of linear elastic spherical particles obeying the Hertz interaction law. These results provide a background for designing strongly nonlinear tunable metamaterials with the ability to increase the sound speed and acoustic impedance by a factor of 3–4 times at very moderate static precompression. This is unattainable for existing solid materials.

References

1. Hopkinson B. 1914 A method of measuring the pressure produced in the detonation of high explosives or by the impact of bullets. *Phil. Trans. R. Soc. Lond. A* **213**, 437–456. (doi:10.1098/rsta.1914.0010)
2. Nesterenko VF. 2001 *Dynamics of heterogeneous materials*, ch. 1, pp. 1–53. New York, NY: Springer.
3. Nesterenko VF. 2003 Shock (blast) mitigation by 'soft' condensed matter. In *Granular material-based technologies* (eds S Sen, ML Hunt, AJ Hurd). Proc. MRS Symp., vol. 759, pp. MM4.3.1–4.3.12. Pittsburgh, PA: MRS Press.
4. Daraio C, Nesterenko VF, Herbold EB, Jin S. 2006 Pulse mitigation by a composite discrete medium. *J. Phys. IV* **134**, 473–479. (doi:10.1051/jp4:2006134073)
5. Daraio C, Nesterenko VF, Herbold EB, Jin S. 2006 Energy trapping and shock disintegration in a composite granular medium. *Phys. Rev. Lett.* **96**, 058002. (doi:10.1103/PhysRevLett.96.058002)
6. Thiel M. 2001 Application of shock waves in medicine. *Clin. Orthop. Relat. Res.* **387**, 18–21.
7. Nesterenko VF, Daraio C, Herbold EB, Jin S. 2005 Anomalous wave reflection at the interface of two strongly nonlinear granular media. *Phys. Rev. Lett.* **95**, 158702. (doi:10.1103/PhysRevLett.95.158702)
8. Coste C, Falcon E, Fauve S. 1997 Solitary waves in a chain of beads under Hertz contact. *Phys. Rev. E* **56**, 6104–6117. (doi:10.1103/PhysRevE.5.6104)
9. Coste C, Gilles B. 1999 On the validity of Hertz contact law for granular material acoustics. *Eur. Phys. J. B* **7**, 155–168. (doi:10.1007/s100510050598)
10. Daraio C, Nesterenko VF, Herbold EB, Jin S. 2005 Strongly nonlinear waves in a chain of Teflon beads. *Phys. Rev. E* **72**, 016603. (doi:10.1103/PhysRevE.72.016603)
11. Daraio C, Nesterenko VF. 2006 Strongly nonlinear wave dynamics in a chain of polymer coated beads. *Phys. Rev. E* **73**, 026612. (doi:10.1103/PhysRevE.73.026612)

Downloaded from https://royalsocietypublishing.org/ on 04 March 2022

12. Herbold EB, Nesterenko VF. 2007 Solitary and shock waves in discrete strongly nonlinear double power-law materials. *Appl. Phys. Lett.* **90**, 261902. (doi:10.1063/1.2751592)
13. Herbold EB, Nesterenko VF. 2007 Solitary and shock waves in strongly nonlinear metamaterials. In *Shock compression of condensed matter* (eds M Elert, MD Furnish, R Chau, N Holmes, J Nguyen). Proc. AIP Conf., vol. 955, pp. 231–243. Melville, NY: AIP Press.
14. Dias IL, Rosas A, Romero AH, Lindenberg K. 2010 Pulse propagation in a chain of O-rings with and without precompression. *Phys. Rev. E* **82**, 031308. (doi:10.1103/PhysRevE.82.031308)
15. Spadoni A, Daraio C, Hurst W, Brown B. 2011 Nonlinear phononic crystals based on chains of disks alternating with toroidal structures. *Appl. Phys. Lett.* **98**, 161901. (doi:10.1063/1.13567753)
16. Gent AN. 2012 *Engineering with rubber*. New York, NY: Hanser.
17. Lindley PB. 1966 Load–compression relationships of rubber units. *J. Strain Anal.* **1**, 190–195. (doi:10.1243/03093247V013190)
18. Allen PW, Lindley PB, Payne AR. 1966 *Use of rubber in engineering*, ch. 1, pp. 1–23. London, UK: Maclaren and Sons.
19. Karpman V. 1975 *Nonlinear waves in dispersive media*, ch. 1, pp. 1–65. New York, NY: Pergamon Press.
20. Herbold EB, Nesterenko VF. 2007 Shock wave structures in a strongly nonlinear lattice with viscous dissipation. *Phys. Rev. E* **75**, 021304. (doi:10.1103/PhysRevE.75.021304)
21. Paterson MS. 1964 Effect of pressure on Young's modulus and the glass transition in rubbers. *J. Appl. Phys.* **35**, 176–179. (doi:10.1063/1.1713063)
22. Huillard G, Noblin X, Rajchenbach J. 2011 Propagation of acoustic waves in a one-dimensional array of noncohesive cylinders. *Phys. Rev. E* **84**, 016602. (doi:10.1103/PhysRevE.84.016602)
23. Lee C-W, Nesterenko VF. 2013 Dynamic deformation of strongly nonlinear toroidal rubber elements. *J. Appl. Phys.* **114**, 083509. (doi:10.1063/1.4819107)